The violin bow: Taper, camber and flexibility

Colin Gough[a]

School of Physics and Astronomy, University of Birmingham, B15 2TT, United Kingdom

An analytic, small-deflection, simplified model of the modern violin bow is introduced to describe the bending profiles and related strengths of an initially straight, uniform cross-section, stick as a function of bow hair tension. A number of illustrative bending profiles (cambers) of the bow are considered, which demonstrate the strong dependence of the flexibility of the bow on longitudinal forces across the ends of the bent stick. Such forces are shown to be comparable in strength to critical buckling loads causing excessive sideways buckling unless the stick is very straight. Non-linear, large deformation, finite element computations extend the analysis to bow hair tensions comparable with and above the critical buckling strength of the straight stick. The geometric model assumes an expression for the taper of Tourte bows introduced by Vuillaume, which is re-examined and generalized to describe violin, viola and cello bows. A comparison is made with recently published measurements of the taper and bending profiles of a particularly fine bow by Kittel.
© 2011 Acoustical Society of America. [DOI: 10.1121/1.3652862]

I. INTRODUCTION

Many string players believe that the bow has a direct influence on the sound of an instrument, in addition to the more obvious properties that control its manipulation on and off the string. It is, therefore, surprising that until relatively recently little research has been published on the elastic and dynamic properties of the bow that might affect the sound of a bowed instrument.

The present paper investigates the influence of the taper and bending profile on the elastic properties of the bow, which could influence the quality of sound produced by the bowed string via their influence on the slip-stick generation of Helmholtz kinks circulating around the vibrating string. The influence of the taper and camber on the flexibility of the bow will also affect the vibrational modes of the bow, to be described in a subsequent paper.

Two scientifically and historically important monographs on the bow were written in the 19th century. The first, by François-Joseph Fétis,[1] was commissioned and published in 1856 by J. B. Vuillaume (1798–1875), the leading French violin maker and dealer of the day. The monograph not only describes and celebrates the instruments of the great Cremonese violin makers, but also gives an account of Vuillaume's own historical and scientific research on the "modern" violin bow. This had relatively recently been developed by Francois Xavier Tourte (1750–1835), who was already viewed as the Stradivarius of bow making.

In 1896, Henry Saint-George[2] updated information on bow makers and described subsequent research on the bow. In addition to translating Vuillaume's earlier research, he describes later research and measurements by the eminent Victorian mathematician W. S. B. Woolhouse, FRS (1809–1893)—the eponymous owner of the 1720 Woolhouse Strad—who collaborated with the distinguished English bow maker James

Tubbs (1835–1921). Woolhouse[3] reflected the views of many modern performers in believing that the *purity* of the vibrations of the bow were as important as the vibrations of the violin itself. Both monographs cite expressions for the taper of fine Tourte bows, but neither indicate how such formulae were derived.

There was then a lengthy hiatus in serious research on the bow until the 1950's. Two interesting papers on the properties of the bow were then published in early Catgut Society Newsletters by Maxwell Kimball[4] and Otto Reder.[5] This was followed in 1975 by a pioneering theoretical and experimental paper on the dynamic properties of the bow and stretched bow hair by Robert Schumacher.[6]

Subsequently, Anders Askenfelt[7–9] at KTH in Stockholm published several important papers on the bow, more recently in collaboration with the distinguished double-bass virtuoso and teacher Knut Guettler.[10,11] Their later publications are mainly devoted to the influence of the bow-string interaction on the sound of an instrument. George Bissinger[12] investigated the mode shapes and frequencies of the bow plus tensioned bow hair and highlighted the importance of the low-frequency bouncing modes, especially for short bow strokes. Such modes have subsequently been extensively investigated by Askenfelt and Guettler.[10]

The present paper is largely devoted to models that describe the static elastic properties of the bow, which provide the theoretical and computational framework to analyze their dynamic properties, as discussed in a subsequent paper.

The paper is divided into three main sections followed by a discussion of the results and a summary.

The first section introduces a small deflection, analytic model for the bending modes of a simplified constant cross-sectional area bow. This illustrates the dependence of bow *strength* (the term used by players to describe the stiffness against bending) on the initial bending profile (camber) and hair tension. Three illustrative cambers are considered equivalent to bending profiles generated by external forces and couples across the ends of the initially straight stick.

---

[a] Author to whom correspondence should be addressed. Electronic address: profgough@googlemail.com

The second section revisits and generalizes Vuillaume's geometric model and related mathematical expression for the tapered diameter of Tourte bows along their lengths. This taper was chosen for the large deformation, non-linear, finite element analysis described in the third section. These computations extend the analysis to longitudinal tensions between the ends of the bent stick approaching and above the critical buckling load of the straight stick ~75 N, comparable in size to typical playing tensions of ~60 ± 5 N (Askenfelt[7]).

For small bending profiles, the finite-element computations reproduce the predictions of the simple analytic model remarkably well, justifying the most important simplifying assumption of the analytic model, but extending the predictions to describe the asymmetries introduced by the tapered stick diameter and more realistic geometries for the frog and head of the bow.

II. A SIMPLE BOW MODEL

A. Introduction to bending of bow stick

The one-dimensional in-plane bending of a tapered bow stick is governed by the bending equation,

$$EI(s)\frac{d^2y}{ds^2} = M(s), \tag{1}$$

where E is Young's modulus along the length of the stick and y and s are the deflections of and distances along the neutral axis. The bending moment $M(s)$ generated by couples and forces acting on the stick will, in general, vary with position along the length of the stick.

$I(s)$ is the second moment of the cross-sectional area

$$\int_{area} y^2 dx dy,$$

which for a constant radius a stick is $\pi a^4/4$. For a stick with octagonal cross-section, $I = 0.055\ w^4$, where w is the width across opposing flat surfaces. For the short, quasi-elliptical, transitional cross-section between the stick and head of the bow, $I = \pi ab^3/4$, where b is the larger, in-plane, semi-axis.

In general, the bending profile will be a function of both the bending moment along the length of the stick and its local radius. When equal and opposite couples are applied across the ends of a constant cross-sectional radius stick, it will be bent into the arc of a circle with radius of curvature $R(s) = (d^2y/ds^2)^{-1} \sim (d^2y/dx^2)^{-1}$, where the approximation ignores second-order, non-linear, corrections in $(dy/dx)^2$. The curvature of a tapered stick will therefore vary along its length—inversely proportional to the fourth power of its diameter.

For a tapered Tourte bow, the diameter of the stick changes from 8.6 mm at the frog end of the bow to 5.3 mm at the tip end (Fétis[1]). When opposing couples are applied across its ends, the curvature will therefore be almost seven times larger at the upper end of the bow than near the frog. Graebner and Pickering[13] suggest that the couple-induced bending profile is the optimum camber for a high quality bow. This suggestion will be assessed in the light of the computations described in this paper.

In the following section, the bending of the bow based on a simplified model similar to that used by Graebner and Pickering is considered. The bow is of length ℓ and constant cross-sectional radius a, with perpendicular rigid levers of height h at each end representing the frog and the head of the bow, between the ends of which the hair is tensioned.

For small bending angles θ, the usual small deflection approximations with $x = s$ measured along the length of the initially straight stick can be made: $\theta \simeq \tan\theta \simeq \sin\theta \simeq dy/dx$, $\cos\theta \simeq 1$ and $R(s) = (d^2y/dx^2)^{-1}$.

B. An analytic model

A linear analysis is assumed similar to that used by Timoshenko and Gere[14] in Chapter 1 of their classic textbook on *The Theory of Elastic Stability*. This provides an invaluable introduction to the bending of straight and bent slender columns like the violin bow, under the combined influence of external moments and both lateral and longitudinal forces.

First consider the bow stick bent by equal and opposite couples and forces of magnitudes C and F across its ends, promoting the upward deflection illustrated in Fig. 1. Imagine a virtual cut across the bent bow at a height y. In static equilibrium, the applied bending couples and forces acting on the separated left-hand section of the stick must be balanced by equal and opposite bending moments and shearing forces exerted on it by the adjoining length of the stick. The bending moment along the length of the stick must therefore vary as $C + Fy$, resulting in a curvature along the length satisfying the bending equation

$$EI\frac{d^2y}{dx^2} = -(C + Fy), \tag{2}$$

which may be written as

$$d^2y/dx^2 + k^2y = -C/EI, \tag{3}$$

where

$$k^2 = F/EI. \tag{4}$$

The influence of longitudinal force on bending profiles of the bow has often been overlooked, though it has a very important influence on the flexibility. This is used to advantage in the *Spiccato* carbon fibre bow[15] developed by Benois Rolland, which has a wire along the central axis of the hollow stick, which can be tensioned to adjust the camber and flexibility to suit the player's preference.

Because the displacement must be symmetrical and zero at both ends, the solutions can be written as
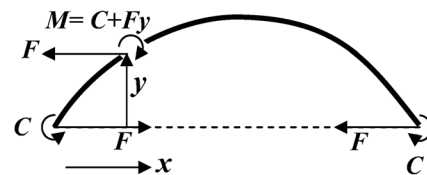

FIG. 1. Equilibrium of bow bent by equal and opposite couples and forces across its ends.

Colin Gough: Violin bow flexibility

$$y = A \sin kx \sin k(\ell - x) \qquad (5)$$

$$= \frac{C}{F} \frac{[\cos k\ell/2 - \cos k(\ell/2 - x)]}{\cos k\ell/2}, \qquad (6)$$

which satisfies the boundary condition $d^2y/dx^2 = -C/EI$ at both ends ($y = 0$).

The maximum deflection at the mid-point is given by

$$y_{\ell/2} = \frac{C\ell^2}{8EI} \frac{2(1 - \cos u)}{u^2 \cos u} = \frac{C\ell^2}{8EI} \lambda(u) \qquad (7)$$

where $u = k\ell/2 = (\ell/2)\sqrt{F/EI}$.

In the above expression, $\lambda(u)$ is essentially a force-dependent factor amplifying the deflection that would have resulted from the bending moment alone, given by the pre-factor in Eq. (7).

The deflection becomes infinite when $k\ell/2 = \pi/2$. This corresponds to a force $F_{Euler} = EI\pi^2/l^2$, which is the maximum compressive load that the straight stick, with hinged supports at both ends, can support without buckling.

For compressive forces F well below the critical limit,

$$\lambda(u) \approx \frac{1}{1 - F/F_{Euler}}, \qquad (8)$$

an approximation that differs from the exact expression by less than 2% for compressive loads below 0.6 of the Euler critical value.

In practice, the bending always remains finite, even for forces well beyond the critical load. This is because, as the bending increases, the two ends of the stick are forced towards each other. The external force then does additional work introducing non-linear terms in the deflection energy analysis, which limits the sideways deflection. This was already understood and mathematical solutions obtained for deflections above the critical load by Euler and Lagrange in the late 18th century (see Timoshenko[16] *History of Strength of Materials,* pp. 30–40).

The neglect of the changes in length between the two ends of the bent stick, limits the above linear analysis to compressive forces significantly smaller than the critical buckling load. Later non-linear finite element analysis shows that the critical buckling tension for a tapered violin stick is around 75 N for pernambuco wood with along-grain elastic constant of 22 GPa. This is only slightly larger than typical bow hair tensions of around 60 N (Askenfelt[7]).

Analytic expressions for large deflection bending were published by Kirchhoff[17] in 1859 based on a close analogy between the bending of a slender column and the non-linear deflections of a simple rigid pendulum. The analytic solutions of what is known as the *elastica* problem involve *complete elliptic integrals* (see Timoshenko and Gere,[14] art 2.7, pp. 76–81). Alternatively, as in this paper, large deflection, non-linear finite element computations can be used to describe such bending, which also allows the influence of the tapered stick and geometry of the frog and head of the bow to be included.

A similar amplification factor applies to any initial sideways bending of the bow stick (Timoshenko and Gere, art 1.12). This explains why bows with only a slight initial

deviation from sideways straightness become virtually unplayable on tightening the bow because of excessive sideways bending. In contrast, the downward curvature of the modern bow is in the opposite sense to that produced by the bow hair tension, which inhibits in-plane instabilities.

When the bending moments are reversed, the sense of deflection is simply reversed. However, reversing the direction of the longitudinal load, $F \rightarrow -F$, has a more profound effect, with $k^2 = F/EI$ now becoming negative. Because $\cos ikx \rightarrow \cosh kx$, the deflections now vary as

$$y(x) = \frac{C}{F} \frac{[\cosh k\ell/2 - \cosh k(\ell/2 - x)]}{\cosh k\ell/2}. \qquad (9)$$

There is no longer a singularity in the denominator. Furthermore, the extensive load now tends to decrease any bending initially present or induced by external couples or forces.

C. Setting of initial camber of bow

In practice, the bow maker adjusts the camber of a bow by bending the stick under a gentle flame. This locks in internal strains equivalent to those that could have been provided by an equivalent combination of couples and forces applied across the ends of the stick or by distributed lateral forces along its length. Timoshenko and Gere,[14] §1.12, provide several examples of the use of such an approach to describe the bending of an initially curved bar.

Bow makers usually assume that a correctly cambered bow should pull uniformly straight along its length on tightening the bow hair (Rolland[18]). They then carefully adjust the bending profile to correct for changes in elastic properties and uneven graduations in taper along the length of the bow. The strength of the bow—the way the stick straightens on tightening the bow hair or deflects on applying downward pressure on the string—will be shown to be strongly related to the camber. Initially, three theoretical profiles will be considered identical to those produced by various combinations of forces and couples across the ends of an initially straight uniform diameter stick.

The earliest suggestion for the most appropriate camber of the modern bow stick was made by Woolhouse[3]:

> Let a bow be made of the proper dimensions, but so as to be perfectly straight; then by screwing it up in the ordinary way, it would show, upside down, the exact curve to which other bows should be set.

This profile will be referred to as the *mirror* profile, as it is the mirror image of the upward bending profile of the tensioned straight stick when inverted. A bow with such an initial camber would indeed straighten uniformly along its length on tightening.

John Graebner and Norman Pickering[13] have recently proposed that the ideal camber would be one generated by equal and opposite couples across the ends of the initially straight stick. Their measurements provide persuasive evidence that this might indeed be true for a number of fine bows. This will be referred to as the *couple* profile. Although such a stick with a uniform diameter would straighten
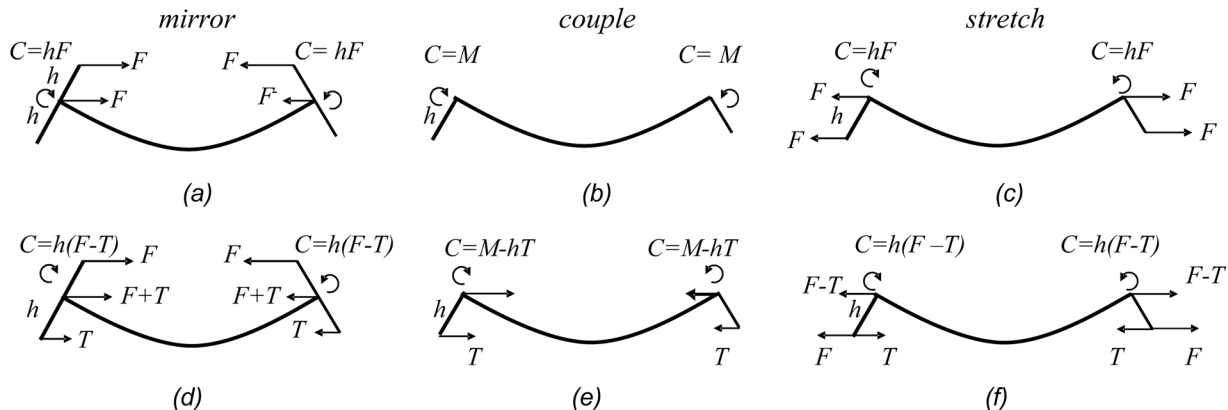
FIG. 2. (a)–(c) illustrate the *mirror, couple* and *stretch* bending profiles generated by equivalent couples and compressive or extensive forces between the ends of the bent stick. (d)–(f) illustrate the additional forces and couples generated by the hair tension T between frog and tip of the bow, with both sets of forces and couples defining the net forces and couples across the ends of the stick determining its bending profile.

uniformly along its length, this is no longer true for a tapered stick. Moreover, such a stick must have a high elastic constant, if it is not to straighten prematurely before a satisfactory playing tensions is achieved.

A profile referred to as the *stretch* profile is also considered equivalent to that produced by an outward force between the ends of the frog and head of the bow, in the opposite direction to the hair tension. It will be shown that a bow with such a bending profile would also straighten uniformly along it length on tightening and would be significantly stronger (less flexible) than bows with *mirror* or *couple* bending profiles.

The equivalent couples and forces used to generate the above three bending profiles are illustrated in Figs. 2(a)–(c), while Figs. 2(d)–(f) illustrate the additional forces and couples generated by the hair tension. These are the only bending profiles that can be generated by couples and forces across the ends of the stick. However, profiles of any desired shape can always be generated by appropriate lateral forces along the length, with the associated bending moments giving the required local curvature [(Timoshenko and Gere[14]), §1.12].

D. Influence of hair tension on bending profile

The deflections of the stick are assumed to be well within the elastic limits of the pernambuco wood used for the stick. The net forces and couples acting across the ends of the stick are therefore the sum of the equivalent forces $\pm F$ and $\pm C$ used to set the untensioned camber plus the forces $\pm T$ and couples $\pm hT$ from the tension of the hair stretched between the end levers representing the frog and head of the bow. However, the deflections from the two sets of forces and couples are not necessarily additive because of the non-linear relationship between the couple-induced deflections and the compressive or extensive loads along the length of the stick.

For the mirror and couple bending profiles under tension, the longitudinal forces are compressive (tensile), so the deflections under tension are given by Eq. (6) with $C = h(F - T)$ and longitudinal force $F + T$ for the *mirror* profile, so that

$$y_{mirror}(T) = \frac{F - T}{F + T} h \frac{[\cos k\ell/2 - \cos k(\ell/2 - x)]}{\cos k\ell/2}, \quad (10)$$

with $k^2 = (F + T)/EI$, and

$$y_{couple}(T) = \frac{M - hT}{T} \frac{[\cos k\ell/2 - \cos k(\ell/2 - x)]}{\cos k\ell/2}, \quad (11)$$

with $k^2 = T/EI$ for the *couple* profile.

For the stretch profile, the net longitudinal forces $(F > T)$ across the ends of the stick are extensive, so that

$$y_{stretch}(T) = h \frac{[\cos k(\ell/2 - x) - \cos k\ell/2]}{\cos k\ell/2}, \quad (12)$$

with $k^2 = (F - T)/EI$.

The camber of the untensioned bow is given by letting $T \to 0$. The resulting cambers for above three bending profiles are shown in Fig. 3, where the equivalent couples C and forces F setting the initial camber have been chosen to give the cited mid-point deflections. For relatively small deflections, the three bending profiles are almost indistinguishable. However, for all deflections, the *couple* bending profile has a slightly larger curvature towards the ends than the *mirror* profile. As the mid-point deflection increases the *stretch* profile becomes progressively flatter in the middle of the bow, as the maximum deflection given by Eq. (12) can never exceed the lever height h, requiring a much larger curvature towards the ends of the bow.

The solid lines in Fig. 4 plot the mid-point deflections as a function of the generating forces and couples used to set the *mirror, couple* and *stretch* profiles for our simple bow model. Note that, although the stresses and strains in the stick are assumed to be elastic, the deflections of the *mirror* and *stretch* profiles are highly non-linear. This is a geometric effect arising from the non-linear amplification of bending profiles by the longitudinal forces as the bending changes [Eq. (2)].

In plotting Fig. 4, a value of EI has been chosen to give a critical buckling load of 78 N, at which force the analytic expression for the *mirror* profile becomes infinite, unphysical and changes sign—indicated by the vertical line. Using this value as the only adjustable parameter, the analytic small deflection predictions for all three bending profiles are almost indistinguishable from the open symbols plotting the
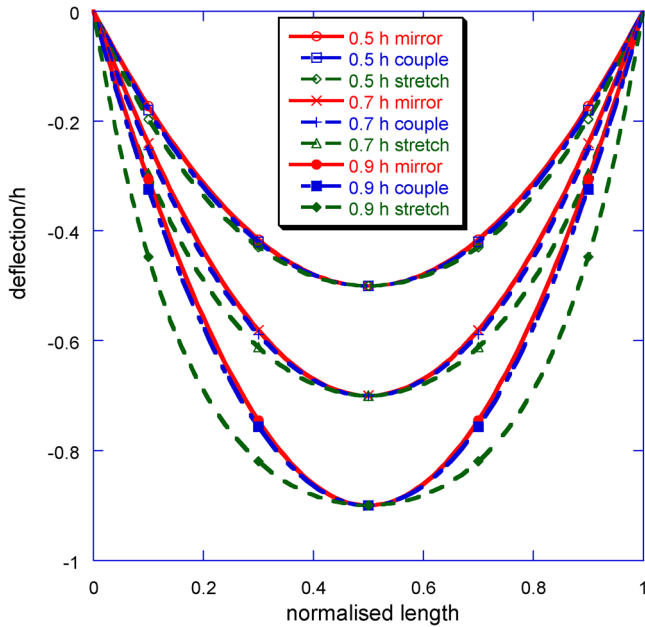
FIG. 3. (Color online) The mirror, couple and stretch bending profiles for mid-point deflections of 0.5, 0.7 and 0.9 the end-lever height h. The model assumes an initially straight bow stick of length 70 cm, with uniform cross-sectional area and $h = 2$ cm.

maximum downward deflections of the tapered Tourte bow computed in Sec. III. Such computations include the changes in geometry, hence bending moments, as the bending increases.

The excellent agreement between the analytic and our later non-linear finite element computations justifies many of the approximations made in the small deflection analysis and justifies its use to illustrate the most important qualitative static and dynamic properties of the bow. Nevertheless, finite-element computations are still required to account for the asymmetric properties associated with the taper and different dimensions of the frog and head of the bow.

Bows with the above bending profiles will straighten when the couples acting on the stick from the hair tension across the frog and tip of the bow are equal and opposite those used to generate the initial untensioned camber. A bow with the *mirror* camber and a downward deflection of 16 mm would therefore straighten with a hair tension of 30 N, only about half the normal playing tension of around 60 N (Askenfelt[7]). A Tourte bow with a *couple* bending profile would also straighten before a playing tension of 60 N could be achieved, unless its elastic constant was significantly higher than 22 GPa or it had a thicker diameter to increase the critical buckling load. In contrast, a bow with a pure *stretch* bending profile could support very large hair tensions without straightening appreciably. Bows of intermediate strength could be produced by setting a camber equivalent to the bending profile produced by a combination of a couple across the bow stick and a stretching force between the frog and head of the bow.

Whatever profile is used by the maker to set the in-plane rigidity, the critical buckling tension of the straight stick must always be significantly larger than the required
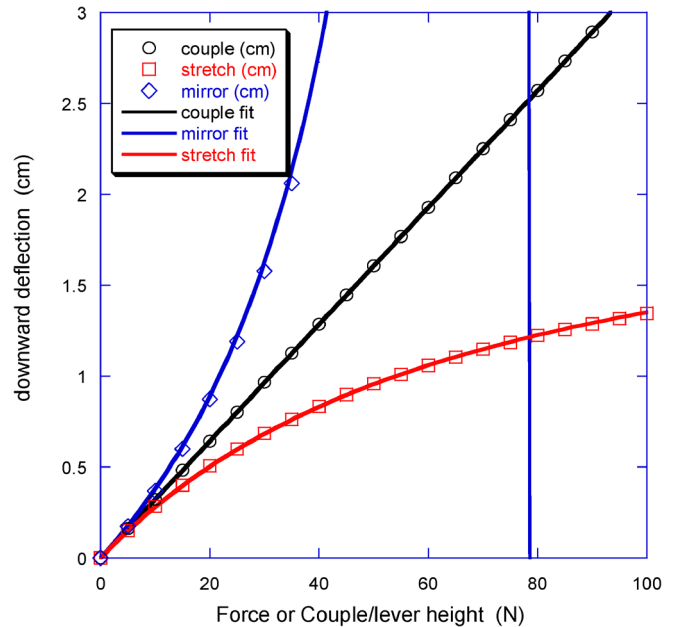

FIG. 4. (Color online) The solid lines represent the bending couples $C = Fh$ and forces F required to set the *mirror, couple* and *stretch* profiles as a function of the mid-point deflection of the 70 cm long, uniform diameter, initially straight stick with $h = 2$ cm levers on its end, for an assumed critical buckling load of $\sim$78 N indicated by the vertical line. The open symbols lying almost exactly on top of the solid lines plot the maximum deflection at around 30 cm from the end of the tapered Tourte stick evaluated using non-linear finite-element software assuming a uniform elastic constant of 22 GPa.

playing tension, to avoid major problems from out-of plane buckling.

The added strength of the *stretch* profile arises from the increased curvature at the ends of the stick, which in a real bow compensates for the loss in bow strength from the reduction in diameter towards the tip. In practice, the bow maker can choose any bending profile they wish and are not constrained to the specific examples considered here. However, for a tapered bow, only the *mirror* or *stretch* bending profiles will pull uniformly straight on tightening the bow hair.

III. THE TAPERED BOW

The taper used in our finite element computations is based on Vuillaume's algebraic expression describing his measurements on a number of fine Tourte bows. Vuillaume noted that all such bows were tapered in much the same way, with the stick diameter decreasing by a given amount at almost exactly the same positions along their length. As cited by Fétis,[1] he therefore devised a geometric construction, so that these positions

might be found with certainty - by which, consequently, bows might be made whose condition should always be settled à priori.

Fétis[1] gives the following mathematical expression,

$$d(x) = -6.22 + 5.14 \log(x + 175), \tag{13}$$

derived by Vuillaume from his geometric model. This gives the tapered diameter d as a function of distance x from the end of the bow stick, with all dimensions in mm.

Unfortunately, no explanation appears to have been given for either the geometric model or mathematical expression derived by Vuillaume and later by Woolhouse[3] from an independent set of measurements on Tourte violin, viola and cello bows.

The Vuillaume geometric model and related mathematical expression have therefore been re-derived and justified. The later Woolhouse expression, as originally correctly cited in mm, is shown to be virtually identical to Vuillaume's earlier expression.

The geometric construction developed by Vuillaume is illustrated in Fig. 5 together with a photograph of a fine Tourte bow and a plot of the tapered diameter on which the geometric model and associated mathematical expression were based.

The bendable length of stick from the frog end to the head of the Tourte bow was measured by Vuillaume as $\ell = 700$ mm, of which the first 110 mm had a constant diameter of 8.6 mm. The remaining 590 mm was tapered towards the upper end with a diameter of 5.3 mm. Vuillaume noted that the tapered section could be divided into 11 sections marking the lengths over each of which the diameter decreased by 0.3 mm, with the length of each section decreasing by the same fraction β, as illustrated schematically in Fig. 5. The decrease in diameter over consecutive sections is therefore described by an arithmetic progression, while the decrease in section length is described by a geometric progression. This forms the basis of Vuillaume's geometric model and related mathematical expression.

The model is generated by first drawing a base line of length 700 mm to represent the length of the stick. At the frog end of the bow a vertical line is raised of height $A = 110$ mm equal in length to the initial constant radius section of the bow. At the other end of the base-line a second vertical line of height B = 22 mm is raised and a straight line drawn between their ends intercepting the axis a distance 175 mm ($\ell/4$) beyond the end of the stick.

A compass was then used to mark out 12 sections along the base line. With the point of the compass at the origin of the base line, a point was first marked off along the base line equal to the height of the first perpendicular representing the initial 110 constant diameter section of the stick. At the end of this section, a new vertical line was raised to intersect the sloping line. Using a compass, this length was added to the first section. The process was then repeated until the remaining sections exactly fitted into the length of the bow stick. The height of the 22 mm upright at the end was chosen so that the fractional decrease in length $\beta = 1 - (A - B)/700 = 0.874$ between successive sections had the correct value to allow this perfect fit. Apart from the initial, constant-diameter, section, each subsequent section marked the lengths over which the diameter decreased by 0.3 mm (3.3 mm in total).

Vuillaume presumably determined the length B by trial and error. Mathematically, this requires the sum of the lengths

$$A \sum_o^{11} \beta^n = 700 \text{ mm},$$

with a ratio of lengths $B/A = \beta^{12} = 22/110 = 1/5$. This gives the above value for β with

$$A \sum_o^{11} \beta^n = 700.5 \text{ mm}$$

and $B = A\beta^{12} = 21.94$ mm, in close agreement with Vuillaume's choice of dimensions for his geometric model.

This simple geometric construction enabled Vuillaume's bow makers to graduate bows with the same taper as Tourte bows. However, it is most unlikely that Tourte would have used such a method. Like all great bow makers, Tourte almost certainly had an innate feeling for the appropriate taper and camber of the bow based on the flexibility of the stick and an aesthetic sense that so often mirrors the elegance and beauty of simple mathematical constructs.

Vuillaume's related mathematical expression for the taper can be derived as follows. From the scaling of triangles with equal internal angles, the distance x_n of the n-th upright from the point of intersection of the sloping line with the base-line satisfies the recurrence formula,
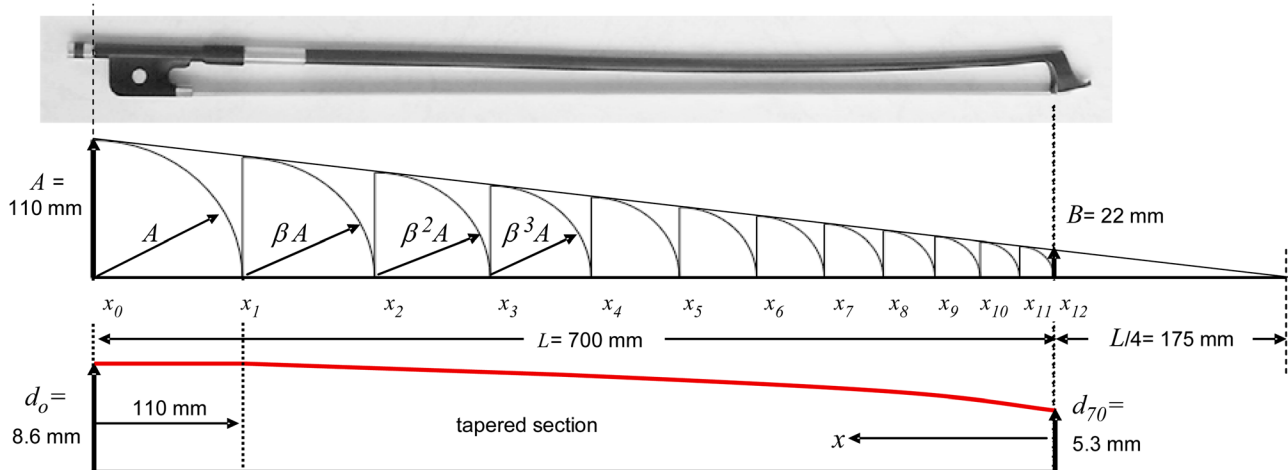

FIG. 5. (Color online) Vuillaume's geometric model reproducing his measurements of the taper of Tourte bows, with a photograph of a bow on the same physical scale and a plot illustrating the functional form of the tapered stick diameter along its length.

$$x_n = \beta x_{n-1}. \tag{14}$$

By iteration,

$$x_n = x_o \beta^n, \tag{15}$$

where x_o is the distance of the far-end of the stick from the point of intersection of the sloping line. Each value of $n > 0$ corresponds to the position along the stick at which the diameter of the following section decreases by $t = 0.3$ mm. The diameter d_n at x_n is therefore given by

$$d_n = d_o - (n-1)t, \tag{16}$$

where d_0 is the diameter of the initial section.

To obtain the algebraic relationship between d_n and x_n, the logarithm is taken of both sides of Eq. (15). The value of n can then be replaced in Eq. (16) to give

$$d_n = (d_o + t) - t[(\log x_n - \log x_0)/\log \beta]. \tag{17}$$

This progression can be described by the continuous function

$$d(x) = C - D \log x, \tag{18}$$

where x is still measured from the point of intersection of Vuillaume's sloping line, 175 mm beyond the end of the stick, $D = t/\log \beta$ and $C - D \log x_1$ is the diameter at the end of the initial 110 mm constant cross-section length ($x_1 = 175 + 700 - 110 = 765$ mm). Insertion of the above parameters in Eq. (18) and redefining x as the distance measured from the head-end of the tapered stick gives

$$d(x) = -6.22 + 5.14 \log(x + 175), \tag{19}$$

with values of the constants essentially identical to those of the Vuillaume expression Eq. (13) cited by Fétis. Note that this formula only applies to the upper 590 mm tapered section of the bow—the lower 110 mm has a constant diameter of 8.6 mm and includes a holding section that is lapped with leather with a metal over-binding to protect the stick from wear.

The mathematical expression replaces the discrete point values of the geometric model with a continuous expression. It is clearly independent of the number of sections over which the changes in diameter were originally measured.

It says much for French education at the time that Vuillaume had the necessary mathematical skills to devise both the geometrical model and the equivalent mathematical expression. It is, of course, likely that he collaborated in their derivation with Felix Savart or some other scientifically trained researcher.

Somewhat later, Woolhouse[3] developed a similar formula based on his independent measurements of the taper of Tourte violin, viola and cello bows. Woolhouse's measurements are tabulated in Saint-George's monograph[2] along with an incorrect expression for the diameter expressed in inches. However, in his original publication, Woolhouse initially cites the diameter in mm as

$$d(x) = -6.17 + 5.08 \log(x + 184), \tag{20}$$

before incorrectly transcribing it into inches. The above expression differs from Vuillaume's expression, Eq. (13), by less than 1% over almost the whole length of the bow, which is almost certainly within the accuracy of their measurements.

It is not obvious why Tourte used the particular taper described above, other than to reduce the weight at the end of the bow without over-reduction of its strength. Other smoothly varying tapers can be devised between fixed upper and lower diameters d_U and d_L of the general form

$$d(x) = d_U + (d_L - d_U)\frac{\log[x/K + 1]}{\log[L/K + 1]}, \tag{21}$$

where L is the length of the tapered section of the bow and K is a scaling distance equivalent to the distance of the point of intersection of the sloping line beyond the end of the bow in Vuillaume's geometric model. K effectively defines the length scale from the end of the bow over which most of the taper occurs. For Tourte bows, the Vuillaume taper parameter $K \sim \ell/4 = 175$ mm, where ℓ is the total bow length.

As K is increased, the taper is more uniformly distributed over the length of the stick, approaching that of a simple truncated cone for large K-values, while smaller values shift the major changes in tapering further towards the tip of the bow. The Woolhouse expression corresponds to a very slightly larger K-value than that derived by Vuillaume.

Figure 6 compares the tapers of fine violin, viola and cello bows measured by Woolhouse[3] and reproduced by Saint-George.[2] The dashed lines drawn through the measured data points are generalized Vuillaume plots, with constants chosen by hand to pass through the measured values. The constants clearly have to be varied to describe the larger
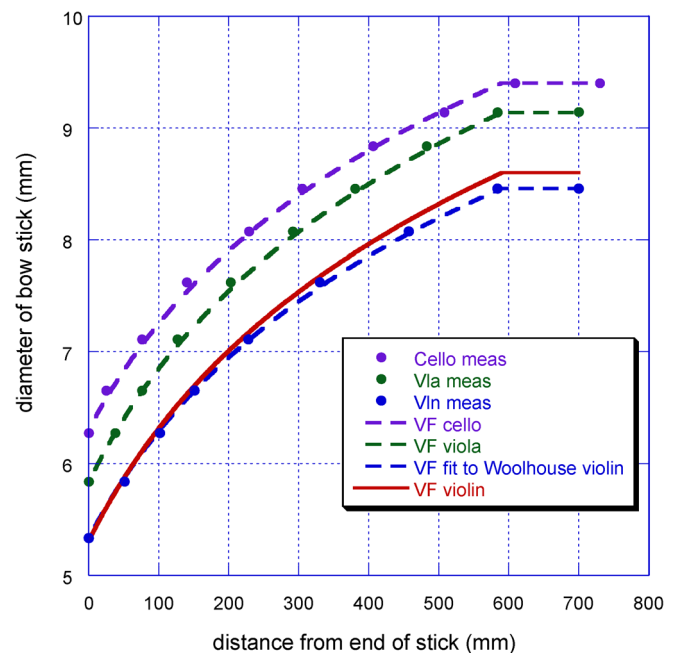

FIG. 6. (Color online) Measured tapers of violin, viola and cello bows by Woolhouse, with dashed lines representing fitted plots of the generalized Vuillaume-Fétis expression for the taper.
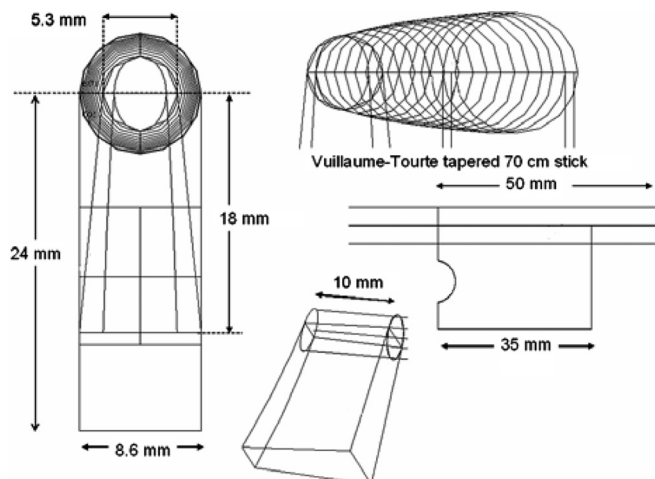
FIG. 7. Finite element geometry of a Tourte-tapered violin bow stick with attached head and frog having effective lever heights from the neutral axis of 18 mm at the head of the bow and 24 mm at the frog.
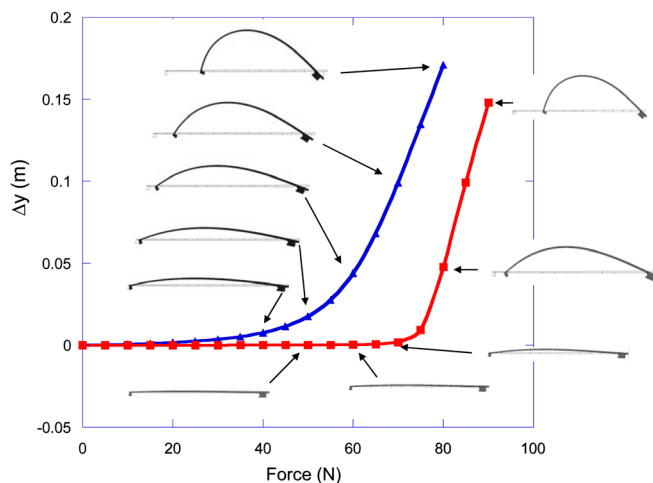

FIG. 8. (Color online) Large-deformation, non-linear, finite-element computations of the deflection of the mid-point of a Tourte-tapered bow stick as a function of hair tension, first applied in the normal way across the ends of the frog and head of the bow and then only slightly offset from the central neutral axis of the stick by the stick radius. The associated bending profiles of the tapered stick are illustrated to exact scale.

diameters and slightly shorter lengths of viola and cello bows, though the general form of the taper remains much the same. Vuillaume derived a very slightly larger thicker section for the bows he measured illustrated by the solid line. The main difference between violin, viola and cello bows is their increasing diameter, hence weight.

IV. FINITE ELEMENT COMPUTATIONS

A. Geometric model and buckling

The Vuillaume expression for the tapered Tourte bow will now be used to describe the taper of our finite-element bow model illustrated schematically in Fig. 7. A uniform elastic constant of $E = 22$ GPa along the grain is assumed. The bow stick was divided into 14, equal-length, conical, sub-domains describing the tapered length of the stick with a crudely modeled rigid bow head and frog at its ends. The bow hair was simply represented by the hair tension between its points of attachment on the underside of the frog and head of the bow.

Because the structure is relatively simple, at least in comparison with the violin, a 3-dimensional analysis of the bending modes was used. Each subdomain was divided into a medium-density mesh resulting in typically ∼10 K degrees of freedom. Deflections were confined to the plane of symmetry passing through the stick, frog and head of the bows. The out-of-plane deflections will be discussed in a later paper on vibrational modes.

The initially straight stick was bent by the same combinations of forces and couples used to set the bending profile of the uniform diameter bow stick. Using COMSOL linear finite element analysis (FEA) software on a modest personal computer, bending profiles for small deflections could be computed in a few seconds, while non-linear analysis, which takes into account all changes in geometry on bending, typically took a few tens of seconds. This increased to several minutes to compute the profile of a stick under the influence of very large bending couples and forces, when the two ends of the bow are forced to move close together.

As an example, Fig. 8 illustrates the bending profiles of an initially straight bow as a function of hair tension applied, first across the ends of the frog and head of the bow in the normal way and then slightly offset from the central stick axis by the radius of the stick. In both cases, the point at which the tension is applied at the frog-end is pinned allowing the bow to rotate, while the tip end of the hair is constrained to move in the direction of the applied tension. The plots illustrate the relative motion of the two ends of the tensioned hair towards each other, while the figures show the associated bending profiles.

For the slightly offset tension, there is very little bending or inward motion of the two ends until the Euler critical load of $T_{Euler} = E\langle I \rangle \pi^2 / L^2 \sim 75$ N is reached. At this tension, there is a fairly sharp transition to the buckled state, with the two ends of the stick forced to move towards each other. $\langle I \rangle$ is the appropriately averaged second moment of the cross-sectional area of the tapered stick. The computations show that the critical load of a straight stick with the Tourte taper is the same as that of a constant radius stick of diameter 6.4 mm—somewhat larger than the 5.3 mm diameter at the tip end of the tapered bow but smaller than the 8.6 mm radius at the frog-end.

In contrast, when the tension is applied across the frog and tip, the couples across the ends of the bow result in a significant amount of bending (buckling) well below T_{Euler}. There is then a continuous transition to the highly buckled state with no sudden instability at T_{Euler}. This is exactly what one would expect, as it corresponds to the drawing up of a simple hunting bow as the string tension across its ends is increased. Because of the additional couple from the lever action of the hair tension acting on the frog and head of the bow, the amount of bending is always larger than the buckling produced by compressive forces across the ends of an initially straight stick. The amount of bending at low hair tension is clearly proportional to the couple from the offset

compressive load, which is determined by the frog and head lever heights.

The non-linear finite element analysis extends the computations to the whole range of possible bending forces and hair tensions, whereas the analytic, small tension analysis is limited to compressive forces across the ends of the bow significantly smaller than T_{Euler}, beyond which the solutions become unphysical.

B. Bending profiles of the tapered stick

The bending of an initially straight Tourte-tapered bow by the same combinations of couples and forces will now be considered using the same *couple, mirror* and *stretch* bending profiles of the constant diameter bow stick described in the earlier analytic section. The *weight* bending profile generated by adding a weight to the mid-point of the horizontal stick is also included, as this is often used by bow makers to assess the strength (rigidity) of the stick.

Figure 9 illustrates the development of the bending profiles as the couples and forces are increased in equal steps over the ranges indicated. The solid lines show the deflections computed using large-deformation, non-linear, finite-element software, while the dashed lines show the computed profiles from linear, finite-element analysis. As a result of the taper, the maximum downward deflection of the stick is shifted to a position about 5 cm beyond the mid-pint of the stick.

The difference between the two sets of computed bending profiles occurs because the linear analysis neglects the changing influence of the longitudinal forces on the stick as the bending changes [Eq. (2)]. This results in non-linear deflections of the bow despite the strains within the stick itself remaining well within the linear elastic limit. The linear analysis only involves the contribution to the bending of the initially straight stick from the couple acting on the stick and not from the longitudinal force, which only contributes to bending once bending has occurred.

The compressive forces across the ends of the bow generating the *mirror* profile enhance any bending already present. This results in a non-linear softening of the bow as the bending is increased. In contrast, the extensive forces generating the *stretch* profile tend to inhibit further increases in bending resulting in a non-linear increase in rigidity of the stick. Such non-linearities are referred to as geometric non-linearities and occur even though the strains within the stick itself remain well within the linear elastic limits.

For the *couple* and *weight* profiles, the deflections are simply proportional to the bending forces, as there are no longitudinal forces giving rise to non-linearity.

The open symbols in Fig. 4 plot the computed maximum downward deflections of the tapered Tourte for the bending forces and couples generating the *mirror, couple* and *stretch* profiles. As remarked earlier, the computed deflections are in excellent agreement with the mid-point deflections predicted by the simple analytic model. The analytic deflections are represented by the solid lines, with forces scaled to give the same critical buckling load. Such agreement is unsurprising, as the deflections—of order the frog and bow head heights—are small compared to the length of the bow stick. The geometric approximations made in the analytic model are therefore well justified. However, finite element computations are necessary to investigate the asymmetries produced by the taper and the different geometries of the frog and head of the bow.

C. Influence of hair tension

Figure 10 illustrates the influence of hair tension on the four bending profiles generated by external couples and forces
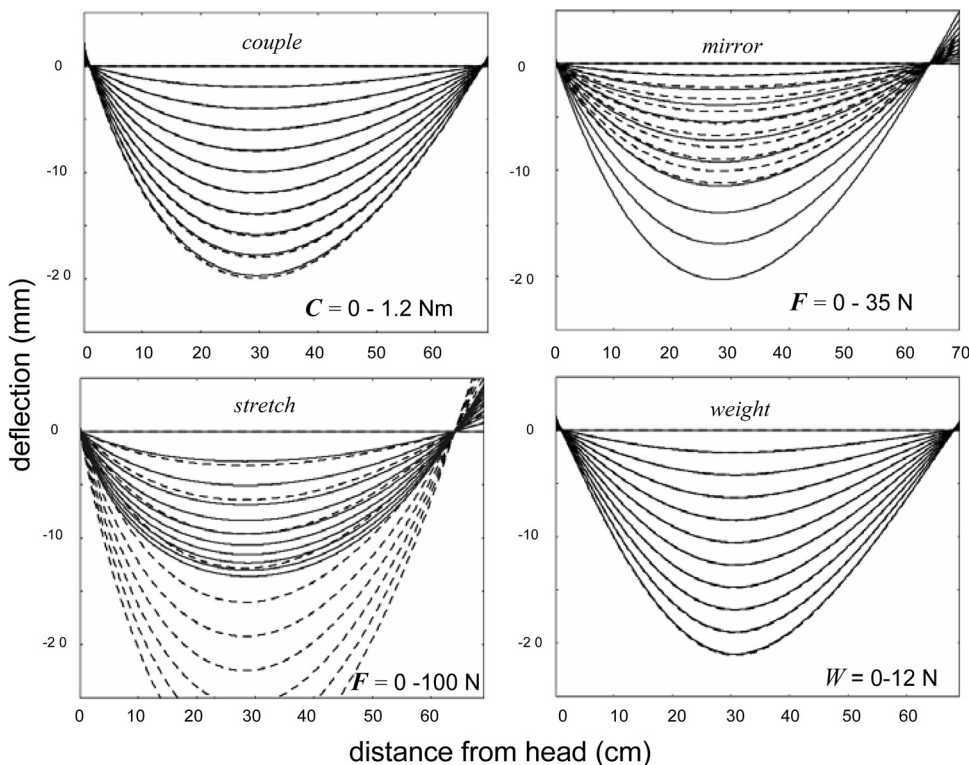

FIG. 9. The dependence of the bending profiles of an initially straight Tourte-tapered bow as a function of the forces and couples used to generate them plotted for equal steps of the forces and couples involved. The dashed lines are the computed profiles computed using linear finite element analysis and the solid lines show the profiles predicted by large-deformation, non-linear computations.
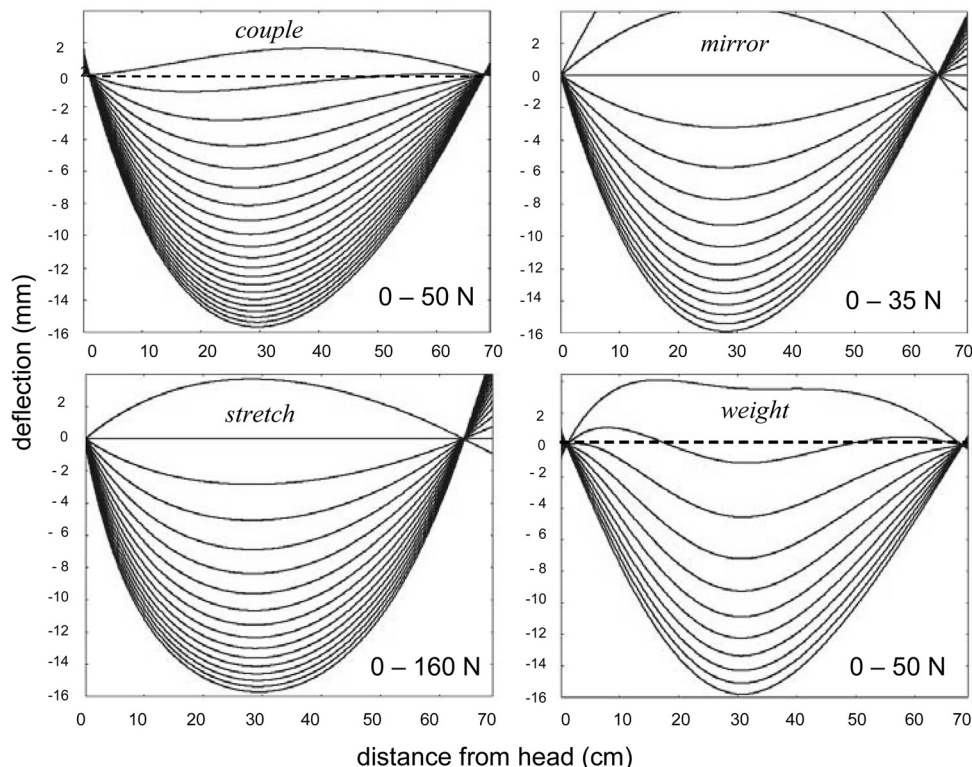
FIG. 10. Straightening of the bow stick on increasing the bow hair tension in equal steps over the indicated range. In each case the forces and couples setting the initial camber of the bow were adjusted to give a typical maximum downward deflection of ~ 16 mm. For the *couple* profile $C = 9.5$ Nm, for the *mirror* profile $F = 50$ N, for the *stretch* profile $F = 190$ N and for the *weight* profile $W = 9$ N.23.

chosen to give a downward stick deflection of ~ 16 mm at around 30 cm from the end of the tapered stick. The plots also highlight the differences in initial bending profiles before the hair tension is applied. For example, the *stretch* profile is very much flatter in the middle of the bow with much more curvature towards its ends than the *mirror* profile, confirming the results for the symmetric, constant radius bow model in Fig. 3.

As expected, a bow with the *mirror* profile is the weakest and pulls "straight" with a hair tension of only ~ 30 N. Bows with the *couple* and *weight* profiles are considerably stronger requiring a hair tension of around 50 N to straighten, while the bow with the *stretch* profile is very much stronger requiring a hair tension of 150 N to straighten. Only tapered bows with *mirror* and *stretch* untensioned cambers straighten uniformly along their length.

The computations confirm that a Tourte taper with a *couple* bending profile would be unable to support a typical hair tension of 60 N unless its along-grain elastic constant was well in excess of the assumed value of 22 GPa. Furthermore, Fig. 10 shows that such a bow would not straighten uniformly on tightening. The computations also confirm that increasing the curvature towards the upper end of the bow increases the strength or rigidity of the bow.

V. DISCUSSION

The bending profiles and resultant flexibilities involve forces and couples that scale with the critical Euler tension $EI\pi^2/\ell^2$. Our model can therefore easily be scaled to viola, cello and double-bass bows, as illustrated by the fitting of the Vuillaume's expression for the taper to Woolhouse's measurements in Fig. 6. Although the scaling clearly depends on the length ℓ of the stick, by far the most important factor is

the r^4 dependence of the second moment of the area I. The larger diameter and slightly shorter viola and cello bows have a significantly larger Euler critical load allowing them to support significantly larger hair tensions without straightening prematurely or buckling sideways.

Until very recently, there were few published measurements of taper and camber curvatures on the same bow to compare with our bending models. However, Graebner and Pickering[13] have recently published such measurements for a number of bows of varying quality including a favorite bow of Heifetz by Kittel (the "German Tourte") of around 1850. Their measurements of bow diameter and curvature are plotted in Figs. 11(a) and 11(b), which also plots the corresponding values for the Vuillaume-Tourte model assuming a *couple* untensioned bending profile (camber). The predicted curvatures proportional to $1/(\text{diam})^4$ have been scaled to take into account differences in densities and elastic constants.

Graebner and Pickering have suggested that the *pure couple* profile represents the optimum camber for a well-made bow. This agrees well with their measurements for the Kittel bow, but less well for many other bows (private communication). In contrast, our computations suggest that a Tourte-tapered bow with a bending profiles generated by couples alone across its ends would be marginally too weak to support today's playing tension of ~ 60 N without pulling straight prematurely—unless the longitudinal elastic constant was well in excess of 22 GPa. This may well be the case for the Kittel bow.

Our analysis shows that, although a uniform diameter bow stick with a *couple* profile would pull straight on increasing the bow hair tension, this is no longer true for a tapered bow. However, it is by no means clear that this would significantly affect the performance of the bow.
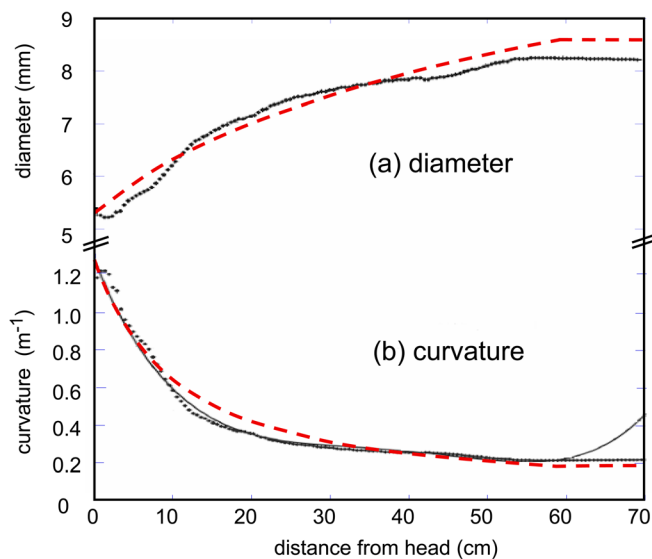
Colin Gough: Violin bow flexibility

FIG. 11. (Color online) Comparisons of (a) the measured diameters (Graebner and Pickering[13]) of a fine bow by Kittel and the Vuillaume-Tourte model and (b) measurements and predictions for the curvature of their cambers assuming couple-induced bending profiles. In (a) the points are Pickering and Graebner's measurements and the dashed curve the Vuillaume-Tourte diameter. In panel (b), the thin solid line passing through the appropriately scaled values of $1/\text{diam}^4$ values was derived from differentiating a 6th-order polynomial fit to the measured bending profile of the Kittel bow (only relevant over the tapered section of the bow); the dashed curve is the predicted Tourte bow curvature.

A detailed comparison between the Graebner and Pickering measurements and the Tourte-tapered bow suggest other possible reasons why a pure couple bending profile may well result in a sufficiently *strong* bow. Figure 11 shows that, although the Kittel bow is slightly thinner than a Tourte tapered bow at its upper end, the diameter increases more rapidly than the Tourte bow and exceed it over a distance of ~20 cm in the upper half of the bow, before decreasing below the Tourte diameter at the frog end. This would account for the difference in curvature from that of the Tourte bow stick shown in Fig. 11(b) potentially giving the bow the added rigidity required to support the hair tension.

Leaving the thinning of the bow to further along the stick corresponds to a decrease in the extrapolation length K in our generalized Vuillaume-Fétis expression for the taper [Eq. (13)]. However, finite element computations suggest that the associated increase in rigidity would be relatively small, only increasing by around 35% for K decreasing from 175 mm to 10 mm, which corresponds to an extremely large difference in taper profile.

VI. SUMMARY

Analytic models and large deformation, finite element computations have been used to investigate the dependence of the flexibility of a Tourte-tapered violin bow on its taper, camber and hair tension.

Representative cambers have been considered generated by various combinations of forces and couples across the ends of the bent stick, both in the untensioned state and with additional couples and forces from the tensioned bow hair. The computations demonstrate that bows of any desired flexibility can always be achieved by a suitable choice of camber, what-

ever the elastic constant of the stick. The often overlooked role of longitudinal forces on the bending profile is highlighted.

In all cases the forces and couples required to produce a given bending profile and rigidity of the bow stick scale with the Euler critical buckling load. The predictions can, therefore, be generalized to describe viola and cello bows. Finite element computations demonstrate that the critical buckling force for a tapered violin bow stick is typically around 75 N, which is not much larger than typical bow hair tensions of around 60 N. This explains why sideways buckling is always a problem for sticks that deviate from straightness or have rather low elastic constants.

The taper assumed for our finite element computations was based on a geometrical model and related mathematical expression originally introduced by Vuillaume to describe his measurements on a number of Tourte bows. This model is re-derived and generalized to describe the tapers of viola and cello bows and shown to be equivalent to a similar expression cited by Woolhouse (after correction for an arithmetic error in the original publication).

Our predictions are compared with recent measurements on a fine bow by Kittel by Graebner and Pickering,[13] who assume the ideal camber for a stick is produced by matched couples alone across the ends of the initially straight stick.

The analytic and computational models developed in this paper provide the theoretical framework for our subsequent analysis of the dynamic modes of the bow stick and their coupled modes of vibration with the stretched bow hair.

[1]F. Fétis, *D'analyses Théoretiques sur l'archet*, in *Antoine Stradivari-Luthiere Célèbre des Instruments a Archet* (Vuillaume, Paris, 1856) (translated as *A Theoretical Analysis of the Bow* in *Anthony Stadivari: The Celebrated Violin Maker* by J. Bishop (Robert Cocks, London, 1864)), http://books.google.co.uk. (Last viewed 09/09/11).

[2]H. Saint-George, *The Bow: Its History, Manufacture and Use*, 3rd ed. (S. A. Kellow, Bridgewater, Somerset, 1923), http://books.google.co.uk. (Last viewed 09/09/11).

[3]W. Woolhouse, "Note on the suitable proportions and dimensions of a violin bow," The Monthly Musical Record, July, 99–100 (1875).

[4]M. Kimball, "On making a violin bow," J. Catgut Acoust. Soc. **11**, 22–26 (1969).

[5]O. Reder, "The search for the perfect bow," J. Catgut Acoust. Soc. **13**, 21–23 (1970).

[6]R. Schumacher, "Some aspects of the bow," J. Catgut Acoust. Soc. **24**, 5–8 (1975).

[7]A. Askenfelt, "Observations on the dynamic properties of violin bows," STL-QPSR **33**, 43–49 (1992), http://www.speech.kth.se/qpsr (Last viewed 09/09/11).

[8]A. Askenfelt, "A look at violin bows," STL-QPSR **34**, 41–48 (1993), http://www.speech.kth.se/qpsr (Last viewed 09/09/11).

[9]A. Askenfelt, "Observations on the violin bow and the interaction with the string," STL-QPSR **36**, 23–42 (1995), http://www.speech.kth.se/qpsr (Last viewed 09/09/11).

[10]A. Askenfelt and K. Guettler, "The bouncing bow: some important parameters," TMH-QPSR **38**, 53–57 (1997), http://www.speech.kth.se/qpsr (Last viewed 09/09/11).

[11]A. Askenfelt and K. Guettler, "Quality aspects of violin bows," J. Acoust. Soc. Am. **105**, 1216 (1999).

[12]G. Bissinger, "Bounce tests, modal analysis, and playing qualities of violin bow," J. Catgut Acoust. Soc. **2**, 17–22 (1995).

[13]J. Graebner and N. Pickering, "Taper and camber of bows," J. Violin Soc. Am. **22**, 160–168 (2010).

[14]S. Timoshenko and J. Gere, *Theory of Elastic Stability*, 2nd ed. (McGraw-Hill, New York, 1961), pages 1–81.

[15]United States Patent: 5,323,675 (June 28, 1984).

[16]S. Timoshenko, *History of Strength of Materials* (McGraw-Hill, New York, 1953), pp. 30–40.

[17]G. Kirchhoff, Journal fur Mathematik (Crelle, Berlin), **56**, 285–313 (1859).

[18]B. Rolland, *The Playing Parts of the Bow: Focussing on the Stick*, J. Violin Soc. Am. **19**(1), 201–217.